Calculation of Brownian Particle Transmission in Long, Wide Channels

Matthew R. Myers
Center for Devices and Radiological Health, U.S. FDA, HFZ-132, Rockville, MD 20852

The transport of Brownian particles in channels which are long and wide compared to their height is addressed. The cross-sectional shape of the channel is assumed to be slowly varying, but otherwise arbitrary. A solution to the convective-diffusive equation with reaction-rate boundary condition was obtained by locally incorporating the modified Graetz solution in a flat channel. The solution was evaluated asymptotically for the cases of a channel with a maximum height occurring at an endpoint and at an interior maximum. The asymptotic method was applied in two example geometries: the calibration apparatus used to determine reaction-rate constants for virus adsorption to latex barriers, and overlapping pores in a nucleation-track membrane. The asymptotic expressions compared well with finite-element calculations in the examples. The utility of the asymptotic approach lies in rapid estimation of particle transmission through a channel as a function of geometric and physical parameters.

Introduction

In a variety of biomedical applications, the transport of Brownian particles through channels which are long and wide compared to the channel height is of interest. An example is the flow of a virus suspension in the gap between human skin and a protective barrier, or the flow of such a suspension through a slit in the protective barrier. It is of considerable practical importance to compute the rate of particle transmission through the channels, after accounting for adsorption of particles to the wall during traversal of the channel. The shape of the channel in the transverse direction is assumed to vary slowly, but the cross-sectional channel shape is otherwise arbitrary.

Particle transport through the channels is characterized by low Reynolds numbers due to the small channel heights (typically submicron to a hundred microns). Owing to the small Brownian diffusivity, though, the Peclet numbers characterizing the transport are large. (See Myers et al., 1999, for a table of parameter values characterizing virus transport through pores in synthetic barriers.) Because the channels are long relative to the channel height, entrance-region solutions are inadequate for computing the quantity of particles exiting the channel.

Away from the channel wall, fluid convection and Brownian motion are the dominant mechanisms of particle transport. Very near the channel wall, colloidal forces between particles and the channel surface become important. When the particle/wall interaction may be adequately modeled by a first-order reaction approximation (Bowen et al., 1976; Van de Ven, 1989; Myers et al., 1999), the particle transport may be described by a convective-diffusion equation in the bulk of the fluid and a first-order-reaction boundary condition at the wall. The problem then becomes equivalent to mass transfer with a permeable boundary (Colton et al., 1971) or heat transfer with constant wall resistance (Sideman et al., 1965).

For special geometries such as parallel-plate and circular cylinder channels, analytical solutions to the governing equations may be obtained using a modified Graetz solution (Bowen et al., 1976). For less-regular geometries, numerical methods may be applied, but it is worthwhile pursuing approximate analytical solutions which clearly manifest the dependence of particle transmission rate upon geometric parameters. In this article we derive an approximate solution to the governing equations to particle transport in a long channel whose shape, assumed unchanging in the axial direction, varies slowly in the transverse direction. We employ a "locally flat" approximation, which utilizes the Graetz solution in a parallel-plate configuration.

The asymptotic solution to the governing equations is derived subsequently. The approximate solution is then applied to two example problems, one in which the maximum channel height occurs at the transverse boundary of the channel and one in which there is an interior maximum. Finally, the

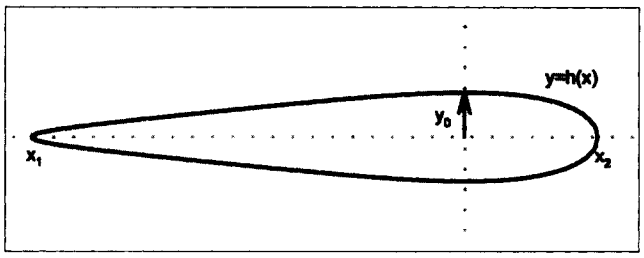

Figure 1. Example cross section illustrating various lengths.

numerical results for the two examples are discussed, and the general accuracy of the asymptotic approach is assessed.

Mathematical Formulation

Consider a channel whose axis coincides with the z-axis, and whose cross-sectional shape is unchanging with z. The maximum channel height, assumed to occur at the transverse coordinate $x = 0$, is $2y_0$. The channel shape in the x-y plane is prescribed by the half-height function $y = h(x)$, $x_1 < x < x_2$, as shown in Figure 1. We assume that the slope $h'(x)$ is small (although this condition can be violated in regions where the channel height is small). It is assumed that particle transport through the channel is adequately described by the convective diffusion equation

$$V\cdot\nabla c - D_\infty\nabla_\perp^2 c = 0, \tag{1}$$

where V is the axial fluid velocity in the channel, c is the particle concentration (particles/vol), D_∞ is the particle diffusivity in an infinite medium, and $\nabla_\perp$ is the gradient operator in the directions transverse to the channel axis (that is, axial diffusion is neglected). The assumptions required for Eq. 1 to apply are discussed in Myers et al. (1999), but perhaps the most critical is that the particle size be much smaller than y_0, in order that the particle velocity be equated to the velocity of the suspending fluid and the diffusivity for an infinite medium apply.

On the channel wall, the "first-order reaction" boundary condition

$$Kc - D_\infty\nabla c\cdot\hat{\boldsymbol{n}} = 0 \tag{2}$$

is applied. Here $\hat{\boldsymbol{n}}$ is the unit normal to the pore wall. The rate-constant K can be written in terms of the potential energy for the colloidal forces (Bowen et al., 1976), but in practice is often determined empirically (Myers et al., 1999). Requiring the slope dh/dx to be small allows the particle near the channel wall to be modeled as residing in the vicinity of a plane, and the near-wall analysis of Bowen et al. (1976) to apply.

We now make further use of the slowly-varying cross-section to find an approximate solution to Eqs. 1 and 2. If dh/dx is small, it is reasonable to ignore diffusion in the x-direction, and to model the geometry at a given x location as locally flat. The velocity and concentration fields can then be approximated by the corresponding quantities for a flat channel. Thus, consider a section of the channel of width dx at location x (dx being large enough to accommodate many particles but much smaller than $x2 - x1$). The particle flux through the subchannel is given by

$$dQ_p = dx\int_{-h(x)}^{h(x)} V(x,y)c(x,y,z)dy. \tag{3}$$

Upon inserting the velocity for fully developed flow in a flat channel (Fox and McDonald, 1978), setting $y' = y/h(x)$, and normalizing the concentration by the channel inlet concentration c_0, we obtain

$$dQ_p = dx\frac{h^3(x)}{2\mu}\left(-\frac{dp}{dz}\right)c_0\int_{-1}^{1}\left[1-y'^2\right]\frac{c}{c_0}dy', \tag{4}$$

where dp/dz is the axial pressure gradient and μ the fluid viscosity. The integral is equal to 4/3 times the mean concentration θ_m for a parallel-plate channel (Bowen et al., 1976). The mean concentration is also identified as the mixing-cup concentration (Colton et al., 1971) in the mass-transfer context and the mixing-cup temperature (Sideman et al., 1965) in heat transfer. After introducing the mean concentration and integrating over the channel width, we arrive at the total particle flow exiting the channel

$$Q_p = \frac{2c_0}{3\mu}\left(-\frac{dp}{dz}\right)\int_{x_1}^{x_2}h^3(x)\theta_m(x,z)dx. \tag{5}$$

The relative particle transmission, equal to the flow of particles exiting the channel divided by the flow entering the channel, is

$$\tau = \frac{\int_{x_1}^{x_2}h^3(x)\theta_m(x,z)dx}{\int_{x_1}^{x_2}h^3(x)dx}. \tag{6}$$

In the modified Graetz solution to Eqs. 1 and 2 in a parallel-plate geometry, the mean concentration can be written as an infinite series of modes (Sideman et al., 1965). For the present purposes, it is convenient to write the series as

$$\theta_m = \sum_1^\infty E_n\exp\left[-\alpha_n R(x,z)\right], \tag{7}$$

where

$$R = \frac{z/V_m}{h^2/D_\infty} \tag{8}$$

is the residence time/diffusion time: the average residence time for a particle in the channel of length z divided by the time for the particle to diffuse the distance h across the channel. Both E_n and α_n are functions of the rate constant K. By incorporating the explicit form for the velocity in a

parallel-plate channel and the diffusivity of a Brownian particle (Probstein, 1994),

$$D_\infty = \frac{kT}{3\pi\mu d} \tag{9}$$

(k being the Boltzmann constant, T the absolute temperature, and d the particle diameter), we obtain for the channel of length L

$$R = \frac{kTL}{\pi d\left[-\left(\frac{dP}{dz}\right)\right]h^4(x)}. \tag{10}$$

The eigenvalues α_n are related to the λ_n of Sideman et al. by

$$\alpha_n = \frac{2}{3}\lambda_n^2. \tag{11}$$

Sideman et al. show that λ_1 and λ_2 differ by approximately 4, and hence α_1 and α_2 vary by more than 10, depending upon the value of K. For the residence time/diffusion time values of interest in long channels [which are O(1) or larger], it is nearly always permissible to retain only the first mode. Using a one-mode expansion of Eq. 7 in Eq. 6, re-expressing $h(x)$ as $y_0H(x)$, and introducing $R_0 = R(x=0)$ yields

$$\tau = \frac{E_1\int_{x_1}^{x_2}\exp\left[3\ln H(x) - \alpha_1 R_0/H^4(x)\right]dx}{\int_{x_1}^{x_2}H^3(x)dx}, \tag{12}$$

where we have also rewritten H^3 as the exponential of a logarithm.

Due to the strong dependence of the exponent in Eq. 12 upon $H(x)$, approximations to the integral can be made based upon the local domination of the integrand by the region near $x=0$. We consider two cases:

(1) $H(x)$ has a maximum at an endpoint, for example, $x_1 = 0$. Expanding the exponent in a Taylor series about $x=0$ and ignoring $O(x^2)$ terms gives

$$E_1\exp[-\alpha_1R_0]\int_0^{x_2}\exp\left[xH'(0)(3+4\alpha_1R_0)\right]dx \tag{13}$$

for the integral in Eq. 12. For sufficiently large values of $x_2|H'(0)|(3+4\alpha_1R_0)$, the upper limit of integration may be set to infinity. Performing the integration yields the final expression for the relative transmission

$$\tau = \frac{E_1\exp[-\alpha_1R_0]}{|H'(0)|(3+4\alpha_1R_0)\int_0^{x_2}H^3(x)dx}. \tag{14}$$

(2) $H(x)$ possesses an interior maximum. We assume $H'(0)=0$, $H''(0)<0$, with $x_1<0<x_2$. Again expanding the exponent in a single-term Taylor series about $x=0$ gives an analogous integral to Eq. 13.

$$E_1\exp[-\alpha_1R_0]\int_{x_1}^{x_2}\exp\left[x^2H''(0)\left(\frac{3}{2}+2\alpha_1R_0\right)\right]dx. \tag{15}$$

For sufficiently large values of the product of $|H''(0)|(\frac{3}{2}+2\alpha_1R_0)$ times x_2^2 and x_1^2, the limits of integration may be set to $\pm\infty$. Upon performing the integration, we can write the relative transmission for the case of an interior maximum

$$\tau = \frac{2E_1\exp[-\alpha_1R_0]}{\int_0^{x_2}H^3(x)dx}\left[\frac{\pi}{(6+8\alpha_1R_0)|H''(0)|}\right]^{1/2}. \tag{16}$$

If multiple maxima occur in the shape function $H(x)$, their contributions may be added in a straightforward way. However, unless the channel height at these locations is very close to y_0, their effect can often be neglected, due to the strong dependence of the integrand in Eq. 12 to channel height.

The procedure for using the asymptotic formulas of Eqs. 14 and 16 is as follows. We assume the channel length, fluid driving pressure, particle diameter, and rate constant are known. Given a channel shape function $h(x)$ with maximum height y_0, the dimensionless rate constant

$$\bar{K} = Ky_0/D_\infty \tag{17}$$

is formed. The table provided by Sideman et al. (1965) and the graph contained in Colton et al. (1971) can be used to determine the constants α_1 and E_1. E_1 varies only slightly, between 0.91 and 1.0, so an average value of 0.955 can be used with little loss of accuracy. For $\bar{K} \gg 1$ the following expression, derived from a perturbation solution to the eigenvalue problem in the flat plate geometry (details available from author), can be used to compute α_1

$$\alpha_1 = 1.88 - 3.23/\bar{K} + O(1/\bar{K}^2). \tag{18}$$

Alternatively, in the empirical determination of K in a parallel-plate geometry, the values of α_1 and E_1 can be derived by plotting relative transmission as a function of residence time/diffusion time. For larger residence time/diffusion time values, the first mode prevails, allowing for direct determination of α_1 and E_1 on a semi-log plot.

The accuracy of the asymptotic formulas is assessed in the following two examples.

Numerical Examples

Exponential cross section

To determine the rate constant characterizing the interaction between viruses and a latex material in a saline medium, parallel vertical sheets were employed in the calibration experiments reported by Myers et al. (1999). A spectrum of residence time/diffusion time values was used; in each experiment R was affected by the clamping compression keeping the sheets together, and determined from the measured fluid-flow rate Q via

$$R = \frac{16kTL}{\pi d\rho g}\left(\frac{12\mu Q}{\rho w g}\right)^{-4/3}. \tag{19}$$

(The channel half-height h is proportional to $Q^{1/3}$ (as in Eq. 4), and, from Eq. 10 R is proportional to h^{-4}.) Here ρ is the fluid density, g is the gravitational acceleration, and w is the

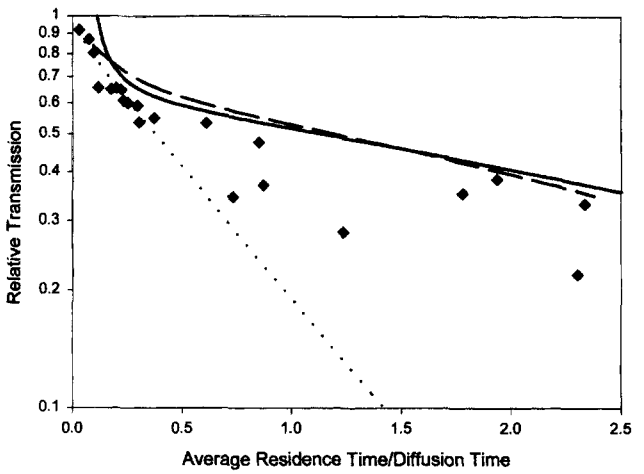

Figure 2. Relative particle transmission as a function of residence time/diffusion time.

Diamonds represent empirical data from the experiments reported by Myers et al. (1999). Dotted line is the predicted transmission under the conditions of these experiments, assuming a flat channel. Solid curve is the asymptotic prediction based upon the same experimental conditions, but assuming a channel of exponential shape. Dashed curve is the finite-element result for the exponential geometry.

channel width. We consider the example of the bacterial virus PRD1 suspended in a medium of 0.16 Molar saline traversing a channel composed of parallel sheets of latex material (Myers et al., 1999). For R less than about 0.4, a close correspondence between empirical values of relative transmission and computed values based upon $k = 0.000285$ cm/s was seen. This correspondence is shown by the data points and the dotted line in Figure 2. (The numerical approach used to compute the results represented by the dotted line is described in Myers et al. (1999). Additional plots in Figure 2 will be discussed subsequently.) However, for larger values of R the computed transmission values were considerably less than the observed ones (Figure 2). Conceivable explanations include that for larger residence times virus desorption or saturation occurs (resulting in higher measured transmission), but these have been dismissed (Myers et al., 2000). Another possible explanation is that the latex material is protruding into the channel, producing a cross section which is not a parallel-sheet geometry. This effect would be exacerbated for smaller channel heights.

To test the effect of a nonrectangular geometry under the conditions reported by Myers et al. (1999), we considered a channel with half-height function of the form

$$H(x) = 0.3 + 0.7\exp(-\beta x), 0 \le x \le w/2, \qquad (20)$$

where $w = 1.0$ cm is the channel width. (The channel is symmetric across $x = w/2$.) We hypothesized that, as clamping compression was applied to the apparatus, rather than the channel height y_0 decreasing to yield higher R values, y_0 stayed constant (at the uncompressed value of the spacers between the sheets, 48 microns) and the sheets simply protruded further into the channel, that is, β increased. In a series of numerical experiments we thus varied β, used the resulting $H(x)$ to compute the flow rate (via Eq. 5 with c_0 and θ_m set to Eq. 1), and then computed R from Eq. 19. At the same time, we computed the full solution to Eqs. 1 and 2 using the Galerkin finite-element method as implemented in the FIDAP commercial software (Fluent Inc., 1998). Details of the finite-element numerical simulation are available from the author. The results for this numerical example are presented in Figure 2. The abscissa is the average residence time/diffusion time for the channel, computed from Eq. 19 (as opposed to the minimum residence time/diffusion time R_0). As noted previously, the experimental data are given by the diamonds, and the theoretical solution based upon a flat channel (of the appropriate compressed height to yield the desired R value) is given by the dotted line. The solid line is the asymptotic result (Eq. 14), based upon $\bar{K} = 20.42$, $\alpha_1 = 1.72$ (from Eq. 18), $E_1 = 0.925$ (from Sideman et al., 1965). The finite-element result is the dashed line.

Overlapping pores in a nucleation-track membrane

As the pore density in a nucleation-track membrane is increased to provide higher filtration rate, the possibility of overlapping pores increases (Brock, 1983). It is therefore desirable to estimate the change in particle transmission rate in the case of overlapping pores. We thus considered channels comprising 2, 3 and 4 overlapping pores, with an individual pore being a circular cylinder and the overlap consisting of one-quarter of the diameter. The cross-section for the two-pore channel is shown in Figure 3. Parameters used in the experiments reported by Lytle et al. (1999) were employed in the calculations: pore radius = $y_0 = 0.1$ micron, diameter of bacterial virus ϕX174 = 27 nm, fluid viscosity (saline) = 0.01 poise, channel length = 10 microns, and driving pressure differential = 57,600 dyn/cm^2. The rate constant K is not reported in Lytle et al. (1999), but a value of $K = 0.0007$ cm/s can be derived (Myers et al., 1999) from the published values of relative transmission for ϕX174 and an SDS-coated polycarbonate filter, with a medium of 0.16 Molar saline. For these parameters $\bar{K} = 0.043$, $\alpha_1 = 0.042$, $E_1 = 1.0$.

In applying the asymptotic formula (Eq. 16) to this channel, it is necessary to account for n maxima, where n is the

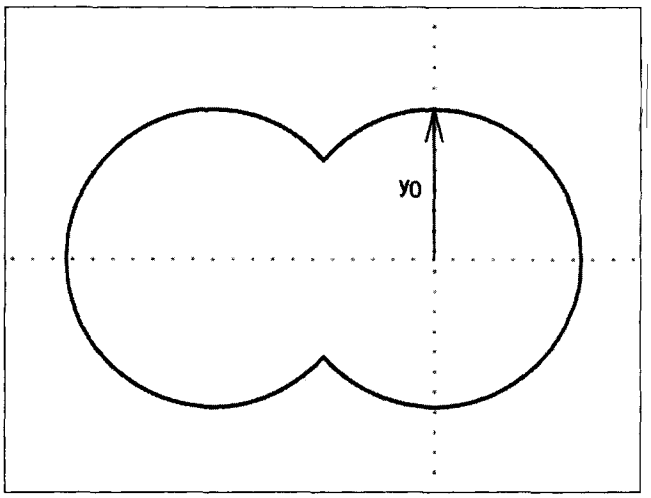

Figure 3. Channel cross section for two overlapping pores in a nucleation-track membrane.

Table 1. Relative Transmission Results for Various Numbers of Overlapping Pores in a Nucleation-Track Membrane*

$\bar{K}$	No. Overlapping Pores	Relative Transmission		
		Finite Element	Asymptotic	Single-Pore
0.043	2	0.32	0.52	0.15
0.043	3	0.38	0.53	0.15
0.043	4	0.42	0.53	0.15
∞	3	0.025	0.13	0.00029

*Computed using the asymptotic approach and the finite-element method within the overlapping-pore channel.

number of circles (2, 3, or 4). Also, given that the wide-channel assumption is only marginally satisfied, a two-term expansion of (Eq. 15) was used. For an elliptical channel, the two-term expansion is obtained by multiplying Eq. 16 by the factor

$$1-\frac{9+36\alpha_1 R_0}{(6+8\alpha_1 R_0)^2}. \tag{21}$$

The asymptotic results {based upon $H(x)=[1-(x/y_0)^2]^{1/2}$, $-0.75y_0 \le x \le y_0$} are compared to the finite-element (FIDAP) calculations in Table 1. For comparison, the relative transmission for a single circular pore (calculated using FIDAP) is displayed in the table as well. Besides the three sets of calculations performed for $\bar{K}=0.043$, an additional comparison was performed in a three-circle channel for a hypothetical virus which is highly absorbing, that is, $\bar{K}=\infty$ ($\alpha_1 = 1.88$). In order to avoid total adsorption of the viruses prior to the channel exit, the pressure differential for this single simulation was increased to 600,000 dyne/cm^2. Results for this high-adsorption situation constitute the last row in Table 1.

Discussion

The close agreement between the finite-element and asymptotic results for the exponential channel (Figure 2) illustrates the usefulness of the simple asymptotic expression (Eq. 14). We note that good accuracy is achieved by the asymptotic result even though its "locally flat" assumption ignores the fact that in reality the velocity goes to zero at the left wall ($x=0$), an effect which is captured by the finite-element simulation. The locally flat assumption also ignores diffusion in the x-direction (contained in the finite-element approach). The slight overprediction by the asymptotic method for larger values of R is possibly due to the emerging importance of transverse diffusion in these steeper channels.

The asymptotic approach formally requires that

$$x_2 \mid H'(0) \mid (3+4\alpha_1 R_0) \gg 1. \tag{22}$$

This criterion is not satisfied for small channel slopes, which correspond to minimal perturbation of the flat geometry by the exponential shape (Eq. 20), and the lowest residence times. The asymptotic result is thus seen to diverge from the finite-element curve at low R values. In general the accuracy of the asymptotic result can be improved by computing more terms in the asymptotic expansion (Eq. 14). However, given the large aspect ratio of this exponential channel [$y_0/(w/2) \approx 0.01$], there is little advantage to expanding the series further.

The plots in Figure 2 demonstrate the plausibility of the hypothesis that the divergence between theory and experiments observed by Myers et al. (1999) was due to a variance from the assumed flat geometry. Despite a slight overprediction by the calculations for the exponential geometry, the empirical trend with increasing R is captured remarkably well. Shapes other than exponential may provide still better agreement with the experimental data. The vast difference in predicted transmission for the flat channel and exponential channel at the same flow rate (or R value) also illustrate the importance of knowing the channel geometry, if accurate predictions of particle transmission are to be made at long residence times and nonzero values of the dimensionless rate constant $\bar{K}$. Hence, knowing only the measured flow rate through the channel, it is typically not possible to arbitrarily model the channel shape and make reliable predictions. Conversely, though, if the channel geometry is not accurately known, the asymptotic expressions (Eqs. 14 and 16) provide a means of rapidly determining the sensitivity of the transmission to geometric and flow parameters. If the channel flow rate is measured, the integral in Eqs. 14 and 16 is known (such as from Eq. 5 with $\theta_m \equiv 1$) and the sensitivity analysis becomes particularly simple.

The overlapping-pores example provides an extreme test of the asymptotic theory. The asymptotic expansion based upon an interior maximum requires

$$x_2^2 \mid H''(0) \mid \left(\frac{3}{2}+2\alpha_1 R_0\right) \gg 1. \tag{23}$$

(and a similar inequality involving x_1^2). For the double-circle pore, the quantity on the lefthand side of the inequality only slightly exceeds 1. The channel is also not very wide relative to its height, even for the 4 circles, making transverse diffusion potentially important. Still, the results in Table 1 are felt to be encouraging for the asymptotic approach. For the 4-circle channel, the asymptotic transmission differs from the finite-element result by only about 20%. Even for the two-circle channel, the asymptotic results qualitatively capture the important effect that the permeability of the filter increases locally in a significant manner when pores overlap. This result is potentially important in filter design. If the number of pores is increased to overcome the flow resistance of the small pores, the relative transmission of the filter increases as the pores begin to overlap.

In the case of the highly absorbing virus, the asymptotic estimate was in error by about a factor of 5. In virus-transport applications, where concentrations are often only known to within an order of magnitude, such accuracy is often acceptable. Also, by comparison, assuming that the transmission rate for the single-pore channel remains valid results in an underestimate of the virus flow by two orders of magnitude.

Conclusion

Simple asymptotic expressions have been presented for calculating Brownian particle transmission through a long, wide channel, in cases where the transport is adequately modeled

by a convective-diffusion equation with reaction-rate boundary condition. The asymptotic approach, when applied to the problem of bacterial-virus transmission through a channel assumed to be of a flat-plate configuration, showed how vast discrepancies between experimental measurements and theoretical predictions can be explained as a strong sensitivity of the transport to variations in the cross-sectional shape. Agreement between the asymptotic result and finite-element calculations was very close, when a perturbation to the flat-plate geometry of an exponential form was considered. The asymptotic method also predicted a large increase in relative virus transmission occurring when two pores in a nucleation-track membrane overlap, a potentially important outcome for filter design. When compared with finite-element calculations, the asymptotic result for the overlapping pores was reasonably accurate, even though the "slowly varying cross section" requirement was barely satisfied. In general, the asymptotic results give insight into the functional dependence of particle transmission on geometric and physical parameters. They can be quickly applied in even complicated geometries, in which considerable time would be devoted to constructing numerical grids. While the formulas were derived in the context of Brownian particle deposition, they can be applied equally well to mass transfer in a permeable channel or heat transfer in a channel with constant wall resistance.

Acknowledgments

Financial support from the Office of Women's Health of the U.S. Food and Drug Administration is gratefully acknowledged.

Literature Cited

Bowen, B. D., S. Levine, and N. Epstein, "Fine Particle Deposition in Laminar Flow through Parallel-Plate and Cylindrical Channels," *J. Colloid Interface Sci.*, **54**, 375 (1976).

Brenner, H., and L. J. Gaydos, "The Constrained Brownian Movement of Spherical Particles in Cylindrical Pores of Comparable Radius," *J. Colloid Interface Sci.*, **58**, 312 (1977).

Brock, T. D., *Membrane Filtration: A User's Guide and Reference Manual*, Science Tech. Publishers, Madison, WI (1983).

Colton, C. K., K. A. Smith, P. Stroeve, and E. W. Merrill, "Laminar Flow Mass Transfer in a Flat Duct with Permeable Walls," *AIChE J.*, **17**, 773 (1971).

Fox, R. W., and A. T. McDonald, *Introduction to Fluid Mechanics*, Wiley, New York (1978).

Fluent, Inc., FIDAP 8 Theory Manual, Fluent, Lebanon, NH (1998).

Lytle, C. D., L. B. Routson, N. B. Jain, M. R. Myers, and B. L. Green, "Virus Passage through Track-Etch Membranes Modified by Salinity and a Nonionic Surfactant," *Appl. Environ. Microbiol.*, **65**, 2733 (1999).

Myers, M. R., C. D. Lytle, and L. B. Routson, "A Mathematical Model for Simulating Virus Transport through Synthetic Barriers," *Bull. Math. Biology*, **61**, 113 (1999).

Myers, M. R., C. D. Lytle, and L. B. Routson, "Virus Adsorption within Pores in Latex: Assessment of Reversibility Effects," *AIChE J.*, **46**, 1894 (Sept. 2000).

Probstein, R. F., *Physicochemical Hydrodynamics*, Wiley Interscience, New York (1994).

Sideman, S., D. Luss, and R. E. Peck, "Heat Transfer in Laminar Flow in Circular and Flat Conduits with (Constant) Surface Resistance," *Appl. Sci. Res. A*, **14**, 157 (1965).

Van de Ven, T. G. M., *Colloidal Hydrodynamics*, Academic Press, San Diego (1989).

Manuscript received Jan. 10, 2000, and revision received June 26, 2000.